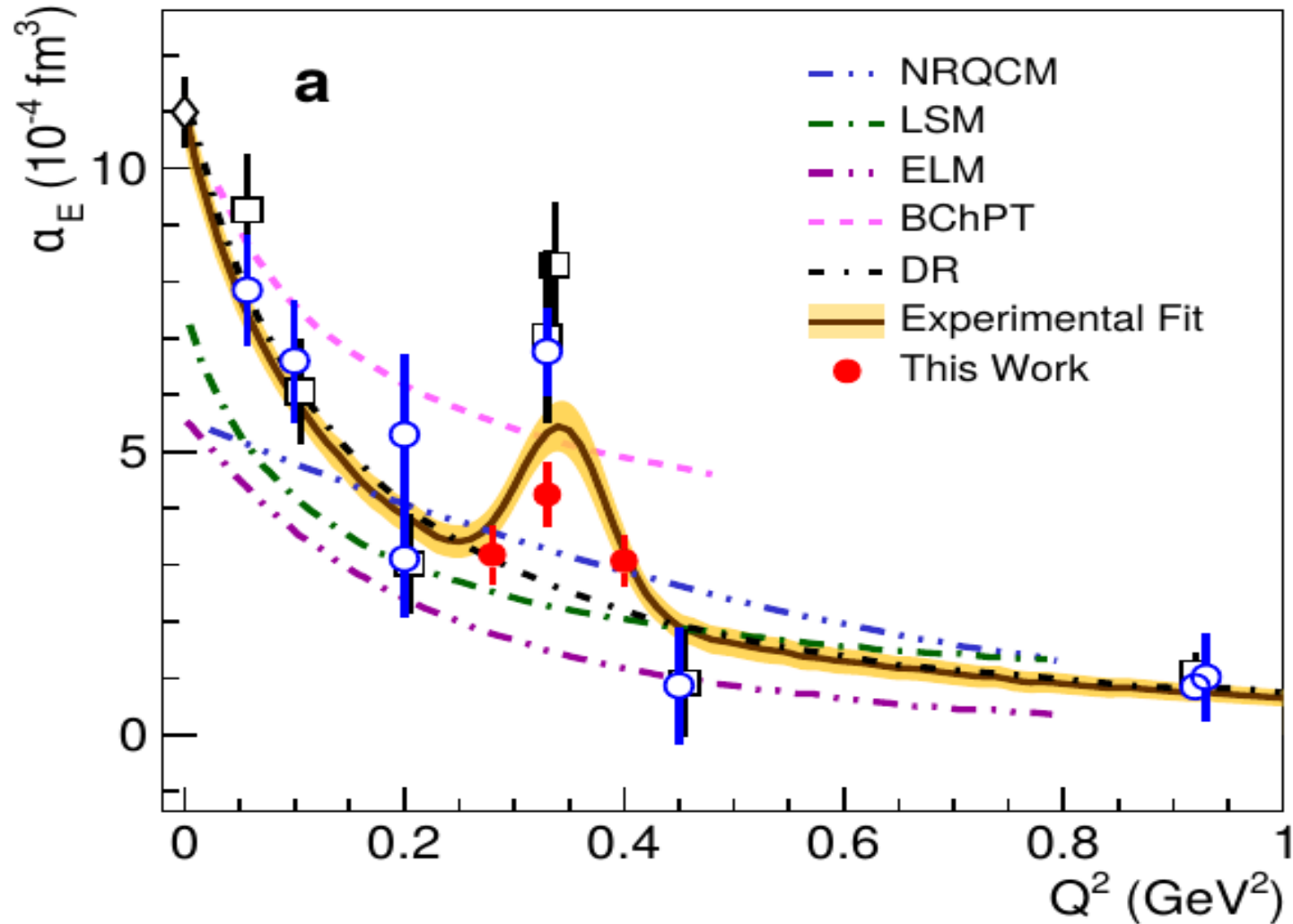


# Measured proton electromagnetic structure deviates from theoretical predictions

2210.11461



# Generalized Polarizability

**JLab confirms the peak at  $Q^2 = 0.33 \text{ GeV}^2$**   
(2210.11461)

1. Definitions and Kinematics
2. Experiment
3. Theor. description
4. Discussion.

Polarizability —

In electric(magnetic) field the system get an additional electric(magnetic) dipole moment

$$d = \alpha_E E \quad (\beta_M H)$$

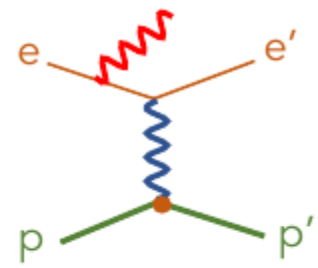
Energy of interaction with this dipole is

$$H_{eff}^{(2)} = -4\pi \left( \frac{1}{2} \alpha_E \vec{E}^2 + \frac{1}{2} \beta_M \vec{H}^2 \right).$$

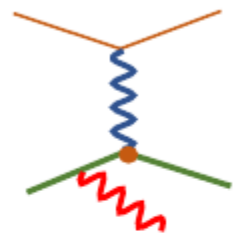
$$\text{since } E \sim qA \quad H_{eff}^{(2)} \propto q^2$$

Since  $H_{eff}^{(2)} \propto A^2 \rightarrow$  search in Compton

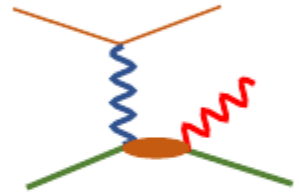
$\gamma p \rightarrow \gamma p$  or  $ep \rightarrow e'p'\gamma$



Bethe-Heitler



Born VCS



non-Born VCS

# Notations:

Incoming

Outgoing

$$\begin{array}{rcl}
 q = k - k' & \begin{array}{l} \text{electron} \\ \text{photon} \\ \text{proton} \end{array} & \begin{array}{l} k' \\ q' \\ p' \end{array}
 \end{array}$$

$$T^{\text{BH}} + T^{\text{Born}} = \frac{b_{-1}(q_{\text{cm}}, \epsilon, \theta_{\text{cm}}, \varphi)}{q'_{\text{cm}}} + \mathcal{O}(q'_{\text{cm}}{}^0),$$

$$T^{\text{NB}} = b_1(q_{\text{cm}}, \epsilon, \theta_{\text{cm}}, \varphi) \cdot q'_{\text{cm}} + \mathcal{O}(q'_{\text{cm}}{}^2)$$

$$d\sigma = d\sigma_{\text{BH+Born}} + \Phi \cdot q'_{\text{cm}} \cdot \Psi_0 + \mathcal{O}(q'_{\text{cm}}{}^2)$$

$$\Psi_0 = V_{LL} \cdot (P_{LL} - P_{TT}/\epsilon) + V_{LT} \cdot P_{LT},$$

$$d\sigma = d\sigma_{\text{BH+Born}} + \Phi \cdot q'_{\text{cm}} \cdot \Psi_0 + \mathcal{O}(q'_{\text{cm}}{}^2) \quad q' \rightarrow 0$$

The next term of the formula,  $(\Phi \cdot q'_{\text{cm}} \cdot \Psi_0)$ , is where the GPs first appear in the expansion.  $\Psi_0$  is the first-order polarizability term, obtained from the interference between the BH+Born and non-Born amplitudes at the lowest order; it is therefore of order  $q'_{\text{cm}}{}^0$ , i.e., independent of  $q'_{\text{cm}}$ . The term  $(\Phi \cdot q'_{\text{cm}})$  is a phase-space factor (see the Appendix for details), in which an explicit factor  $q'_{\text{cm}}$  has been factored

$$\Psi_0 = V_{LL} \cdot (P_{LL} - P_{TT}/\epsilon) + V_{LT} \cdot P_{LT}$$

$$V_{LL} = 2K_2 \cdot v_1 \cdot \epsilon$$

$$V_{LT} = 2K_2 \cdot (v_2 - \frac{\tilde{q}_{0\text{cm}}}{q_{\text{cm}}} \cdot v_3) \cdot \sqrt{2\epsilon(1 + \epsilon)}$$

$$P_{LL}(0) = \frac{4M_N}{\alpha_{QED}} \cdot \alpha_{\text{E1}}(0)$$

$$P_{TT}(0) = 0$$

$$P_{LT}(0) = \frac{-2M_N}{\alpha_{QED}} \cdot \beta_{\text{M1}}(0)$$

$$\epsilon = 1/[1 + 2\frac{q_{\text{lab}}^2}{Q^2} \tan^2(\theta'_{e\text{lab}}/2)]$$

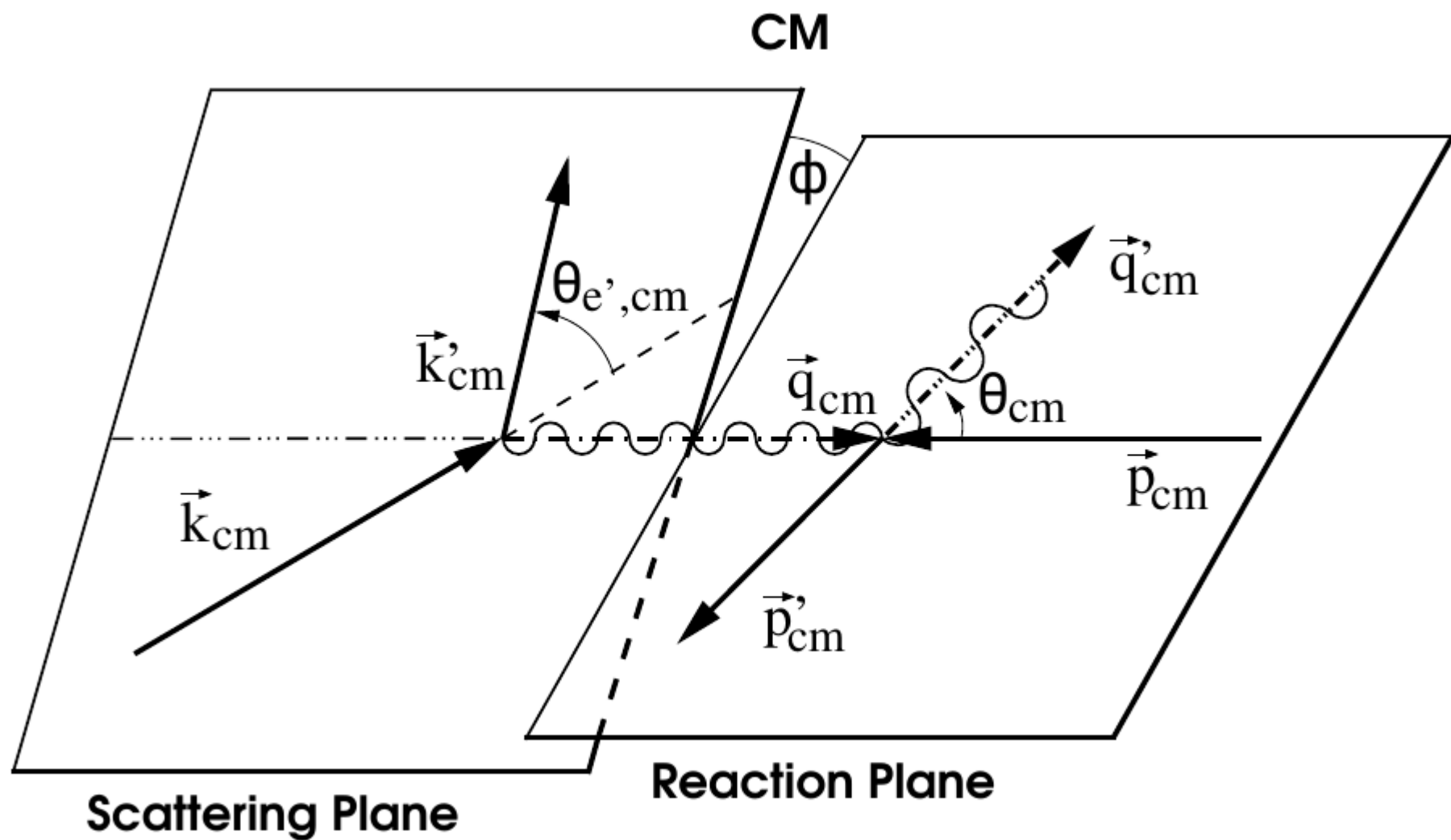
$$K_2 = e^6 \frac{q}{\tilde{Q}^2} \frac{2m}{1 - \varepsilon} \sqrt{\frac{2E_q}{E_q + m}}, \quad E_q = \sqrt{m^2 + q^2}.$$

The angular dependent functions  $(v_1, v_2, \dots)$  are given by

$$v_1 = \sin \theta \left( \omega'' \sin \theta - k_T \omega' \cos \theta \cos \phi \right),$$

$$v_2 = - \left( \omega'' \sin \theta \cos \phi - k_T \omega' \cos \theta \right),$$

$$v_3 = - \left( \omega'' \sin \theta \cos \theta \cos \phi - k_T \omega' \left( 1 - \sin^2 \theta \cos^2 \phi \right) \right),$$

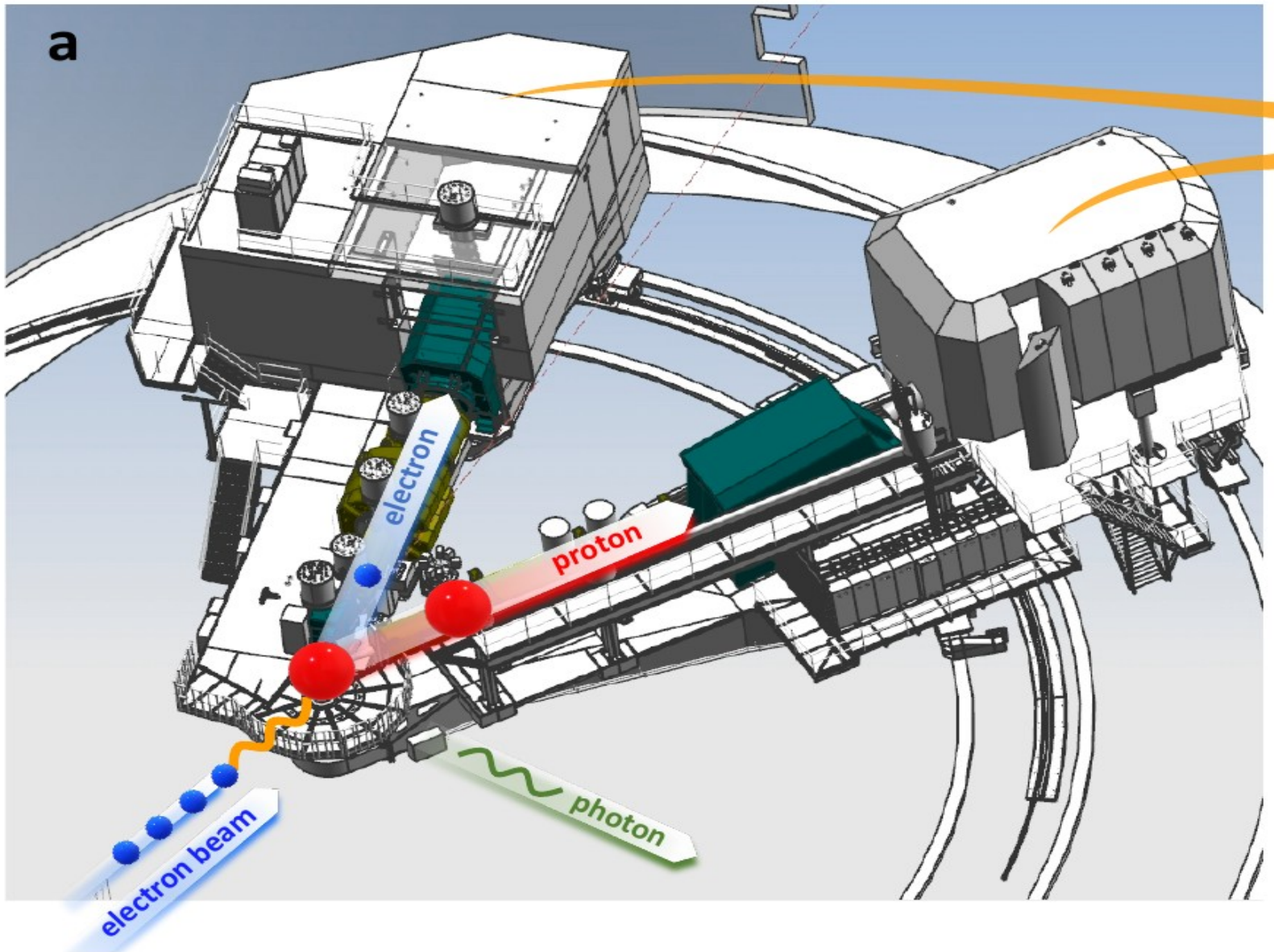




$P^{(\rho'L',\rho L)S}(q_{\text{cm}})$	$P^{(f,i)S}(q_{\text{cm}})$	RCS limit ( $Q^2 \rightarrow 0$ )
$P^{(01,01)0}$	$P^{(L1,L1)0}$	$-\frac{4\pi}{e^2} \sqrt{\frac{2}{3}} \alpha_{E1}$
$P^{(11,11)0}$	$P^{(M1,M1)0}$	$-\frac{4\pi}{e^2} \sqrt{\frac{8}{3}} \beta_{M1}$
$P^{(01,01)1}$	$P^{(L1,L1)1}$	0
$P^{(11,11)1}$	$P^{(M1,M1)1}$	0
$P^{(01,12)1}$	$P^{(L1,M2)1}$	$-\frac{4\pi}{e^2} \frac{\sqrt{2}}{3} \gamma_{E1M2}$
$P^{(11,02)1}$	$P^{(M1,L2)1}$	$-\frac{4\pi}{e^2} \frac{2\sqrt{2}}{3\sqrt{3}} \gamma_{M1E2}$

# Experiment

JLab



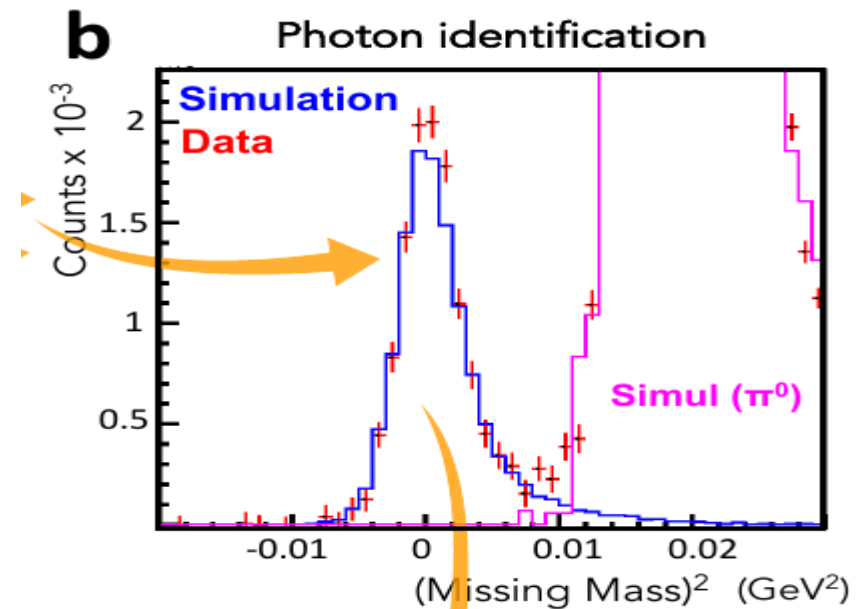
4.56 GeV at a beam current up to  $20 \mu\text{A}$   
10 cm long liquid-hydrogen target at a temperature of 19 K  
 $\mathbf{q} = \mathbf{k} - \mathbf{k}'$ , with  $Q^2 \equiv -\mathbf{q}^2$ .

Time coincidence 1 nsec

time-of-flight proton identification (scintillators)

drift chambers to provide the tracking

$ep \rightarrow e'p'\pi^0$  to control normalization.



Drawback –  $q' \sim 250$  MeV (not small)  
 $\Delta$ -isobar region

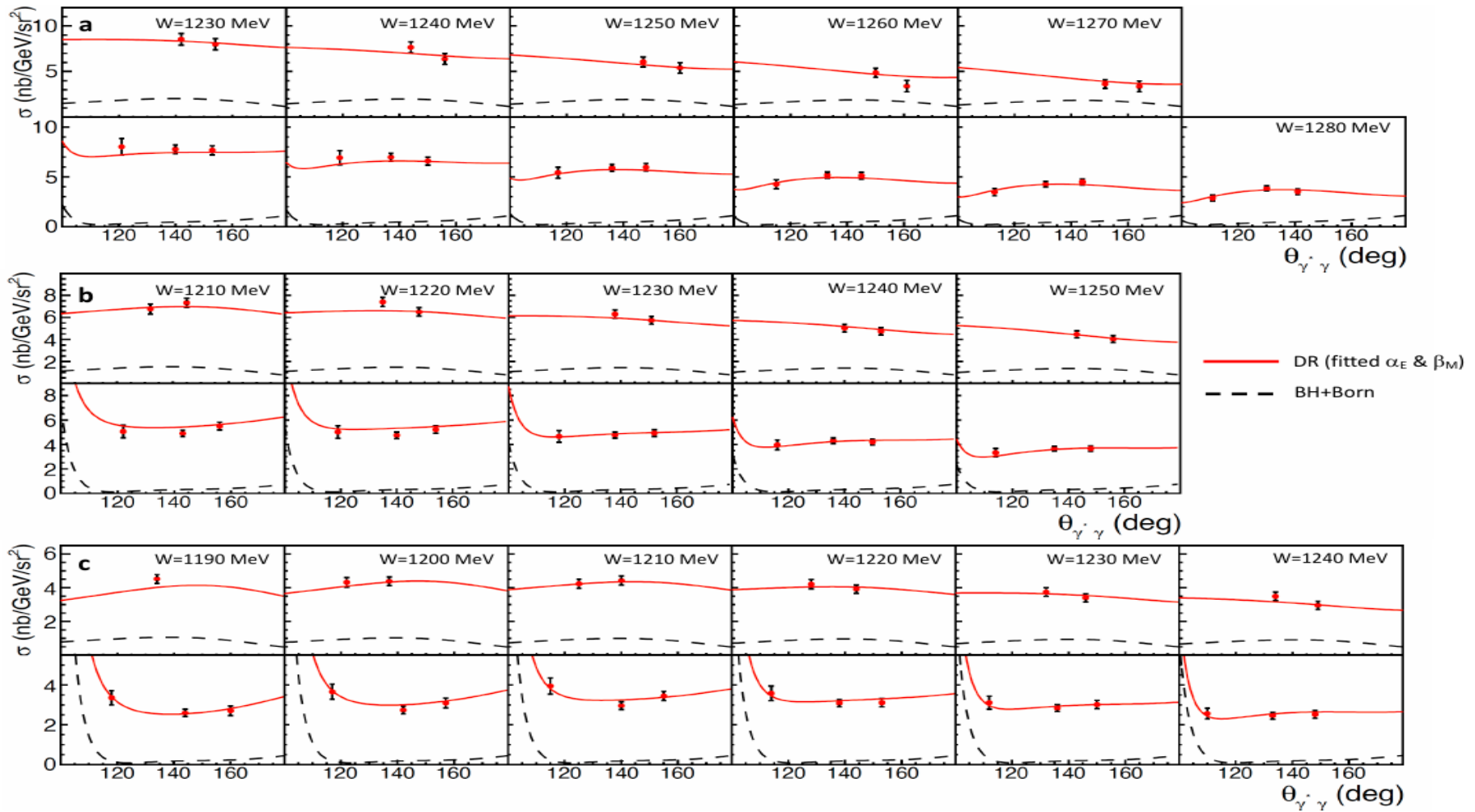
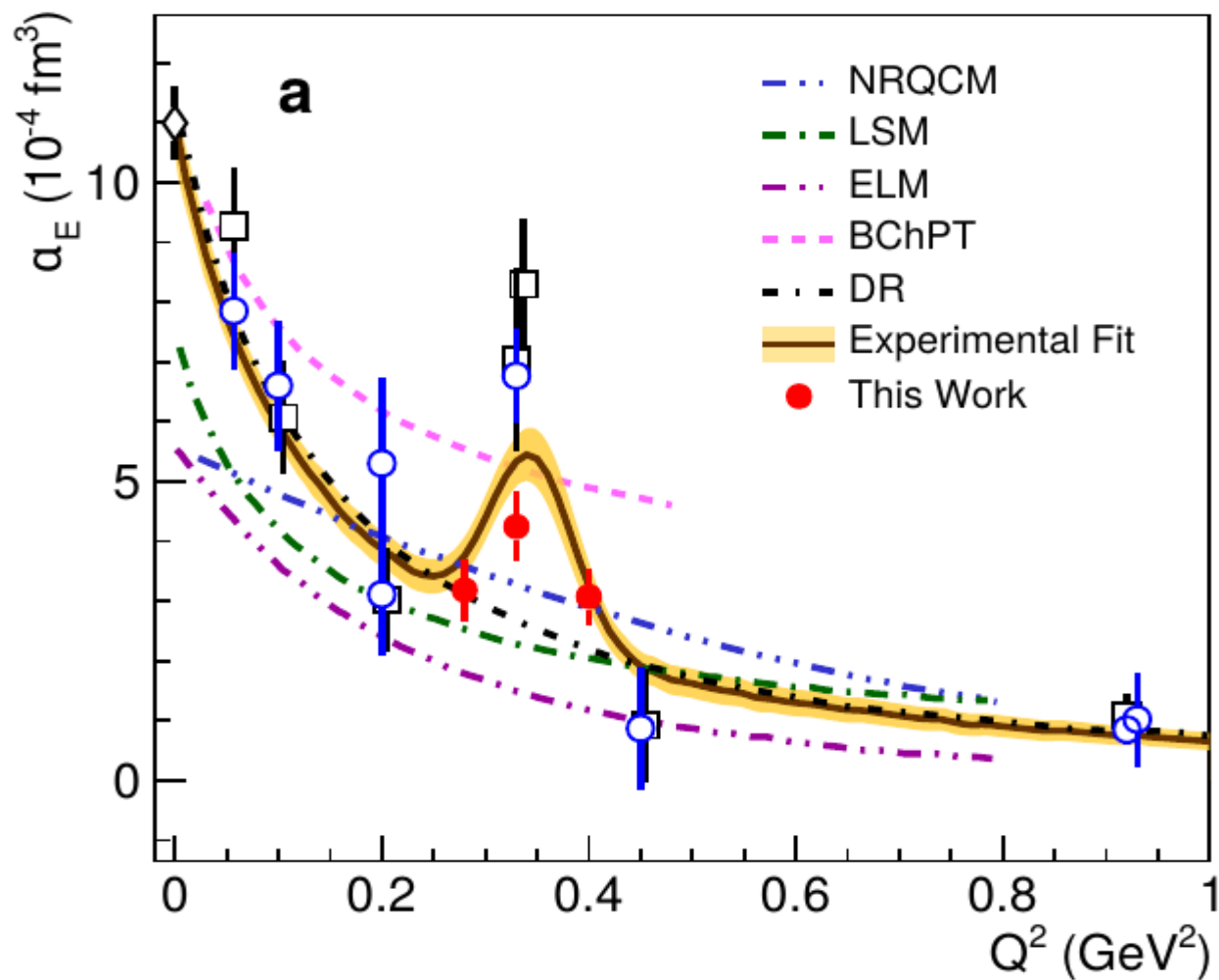


**Figure 3. Cross section measurements of the VCS reaction**

**a)** Cross section measurements for in-plane kinematics at  $Q^2=0.28 \text{ GeV}^2$ . Results are shown for different bins in the total c.m. energy,  $W$ , of the  $(\gamma p)$  system. **b)** Measurements for in-plane kinematics at  $Q^2=0.33 \text{ GeV}^2$ . **c)** Measurements for in-plane kinematics at  $Q^2=0.40 \text{ GeV}^2$ . Top and bottom panels correspond to  $\phi_{\gamma^* \gamma} = 180^\circ$  and  $\phi_{\gamma^* \gamma} = 0$ , respectively. The solid curve shows the Dispersion Relation (DR) fit for the two scalar generalized polarizabilities. The dashed curve shows the Bethe-Heitler plus Born-VCS (BH+Born) cross section. The error bars correspond to the total uncertainty, at the  $1\sigma$  or 68% confidence level.



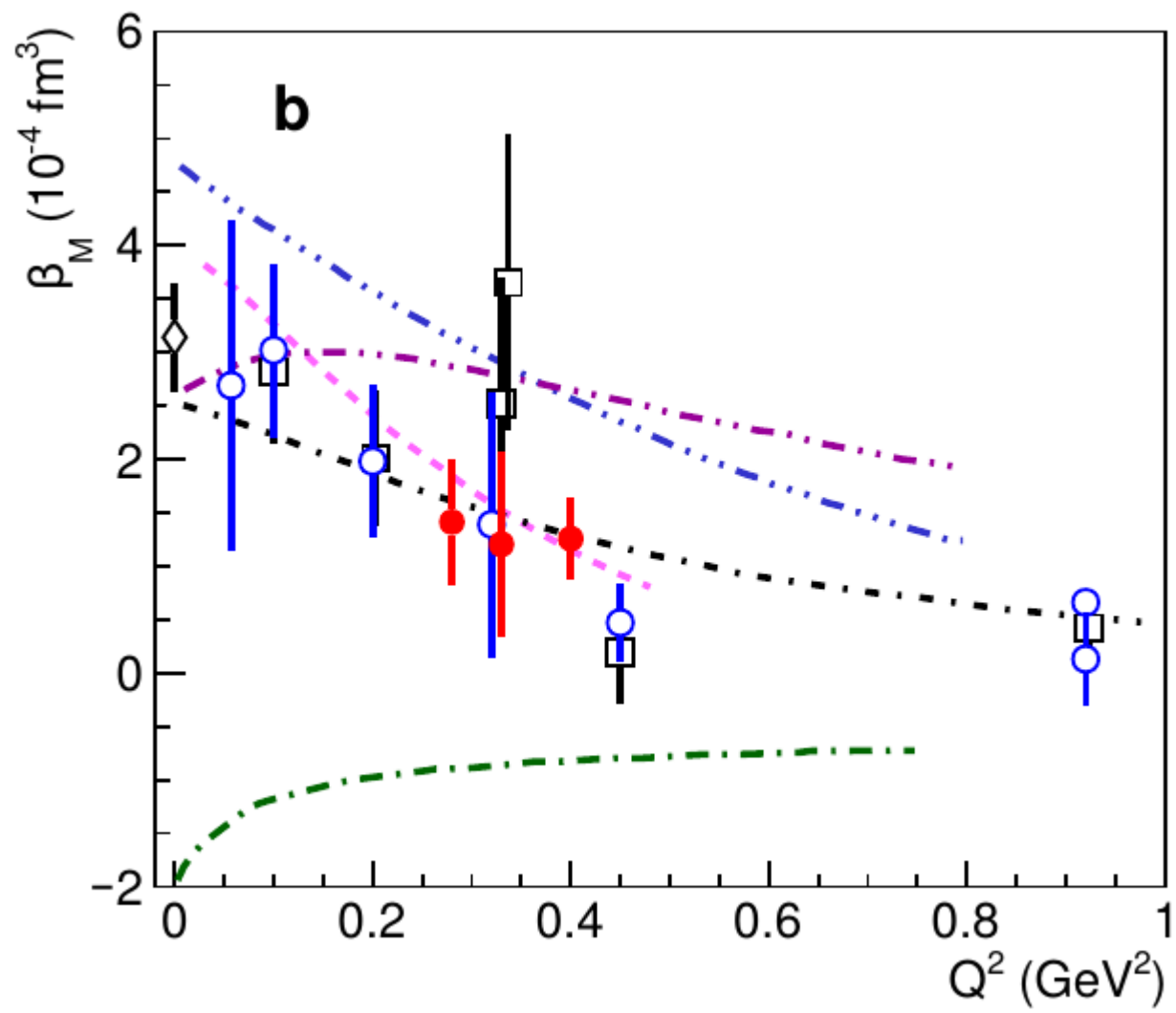
NRQCM – constituent quark model

LSM – linear sigma model

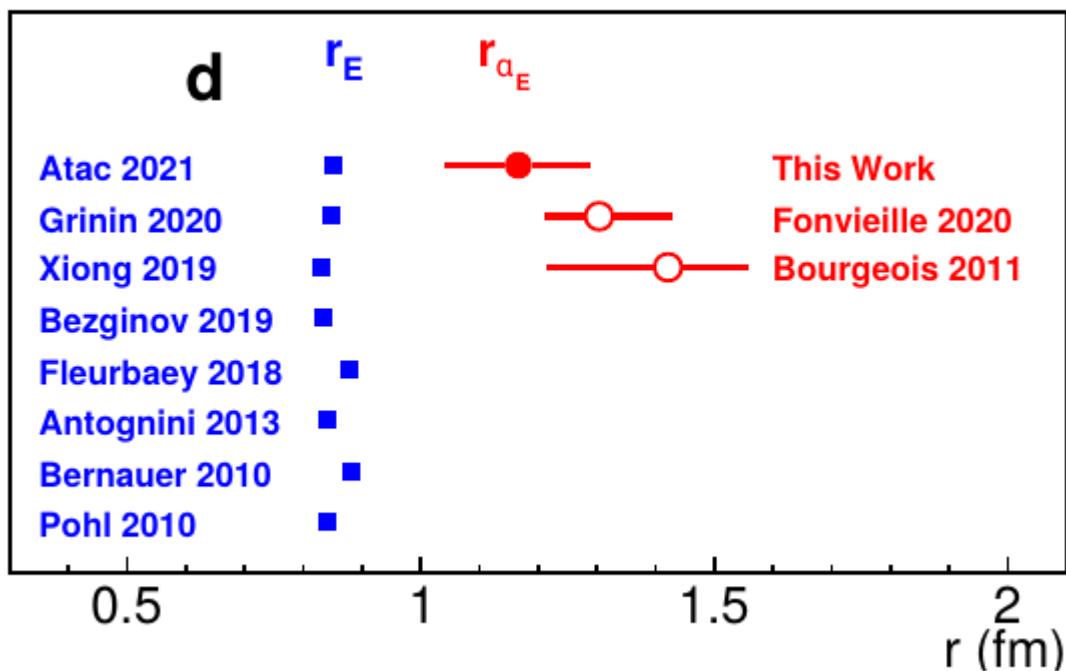
ELM — effective Lagrangian

BChPT – chiral perturbative

DR – dispersion relations



$$r_{\alpha_E} \equiv \sqrt{\langle r_{\alpha_E}^2 \rangle}$$



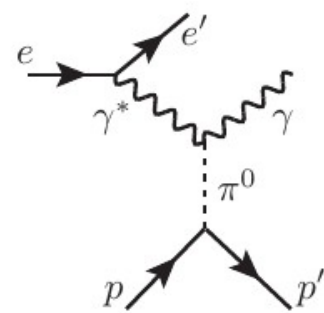
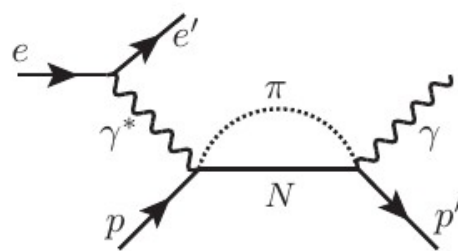
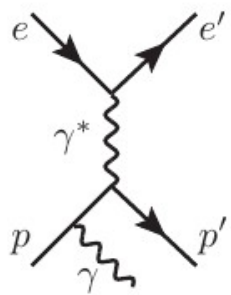
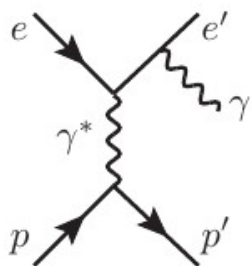
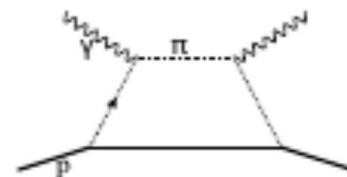
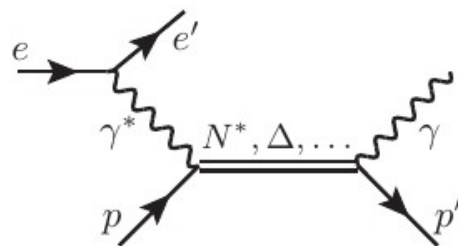
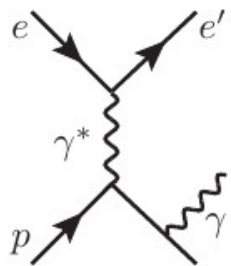
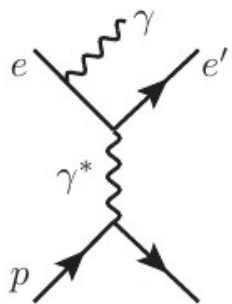
$$\langle r_{\alpha_E}^2 \rangle = \frac{-6}{\alpha_E(0)} \cdot \frac{d}{dQ^2} \alpha_E(Q^2) \Big|_{Q^2=0}$$

$$\langle r_{\alpha_E}^2 \rangle = 1.36 \pm 0.29 \text{ fm}^2$$

$$\langle r_{\beta_M}^2 \rangle = 0.63 \pm 0.31 \text{ fm}^2$$

$$\langle r_E^2 \rangle \sim 0.7 \text{ fm}^2$$





Bethe-Heitler

VCS Born

VCS non-Born

$\pi^0$  pole

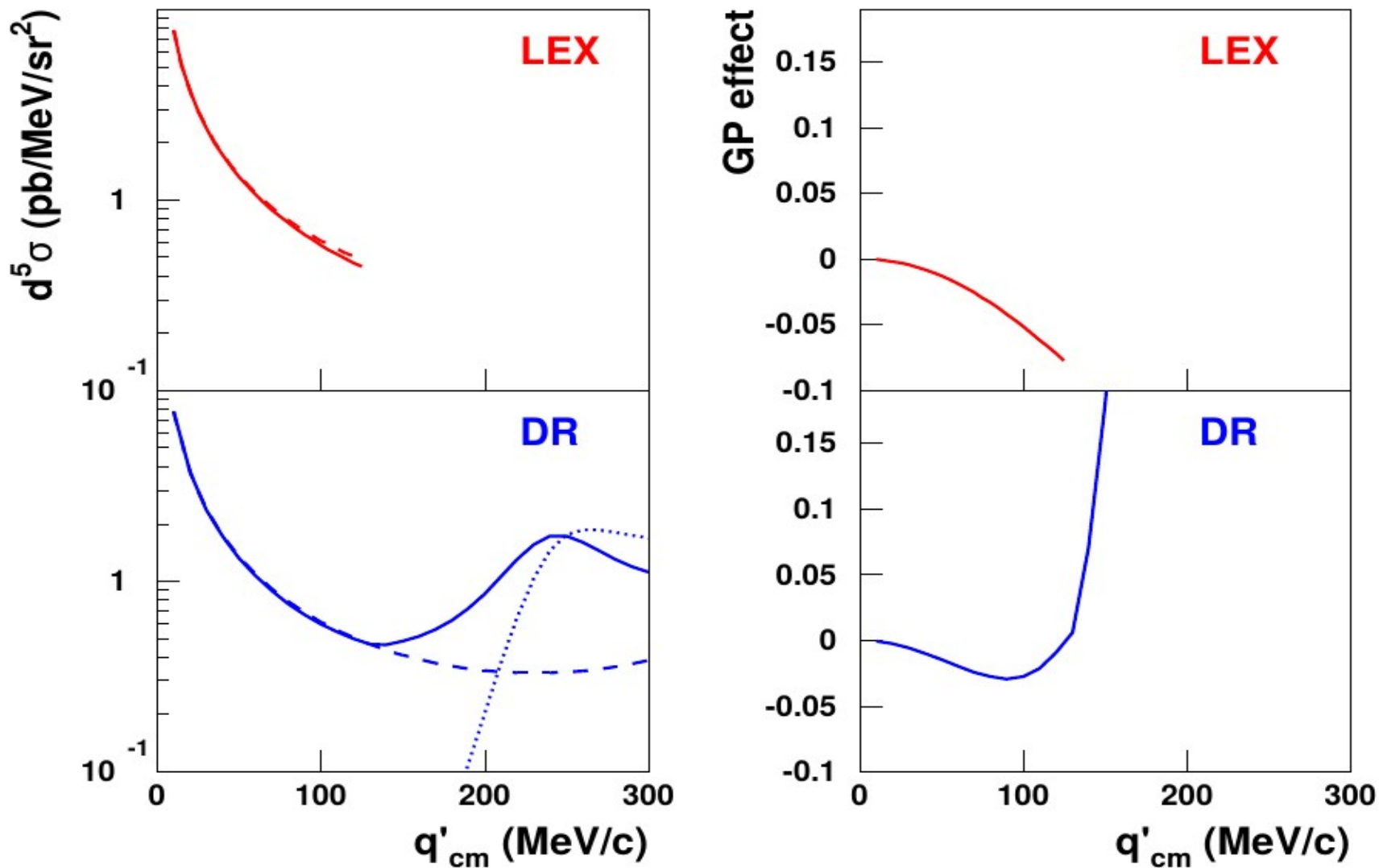
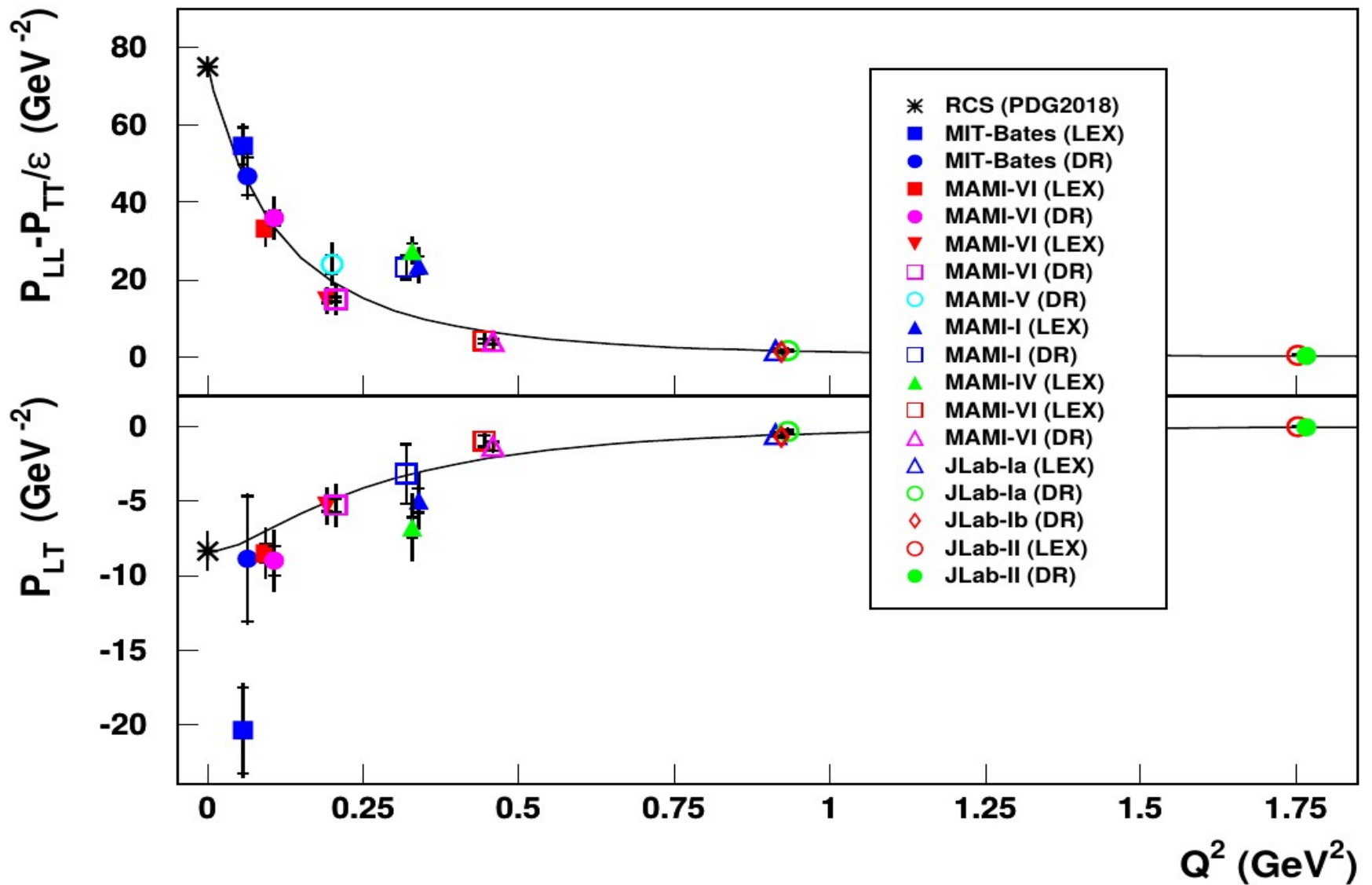
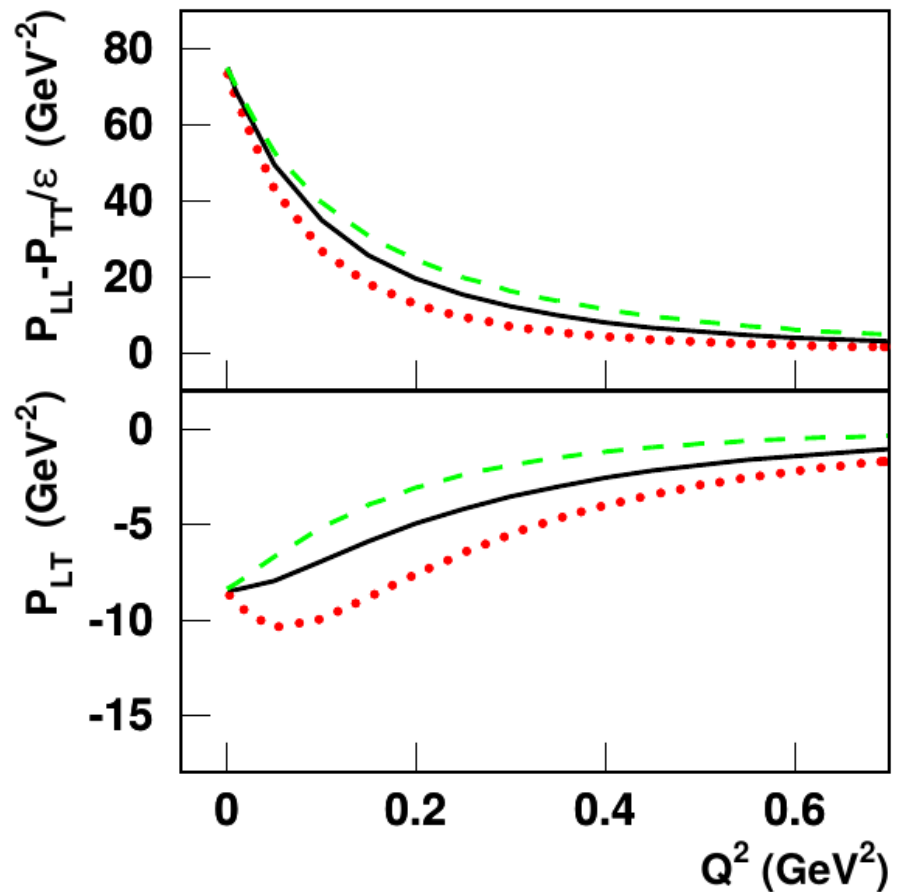
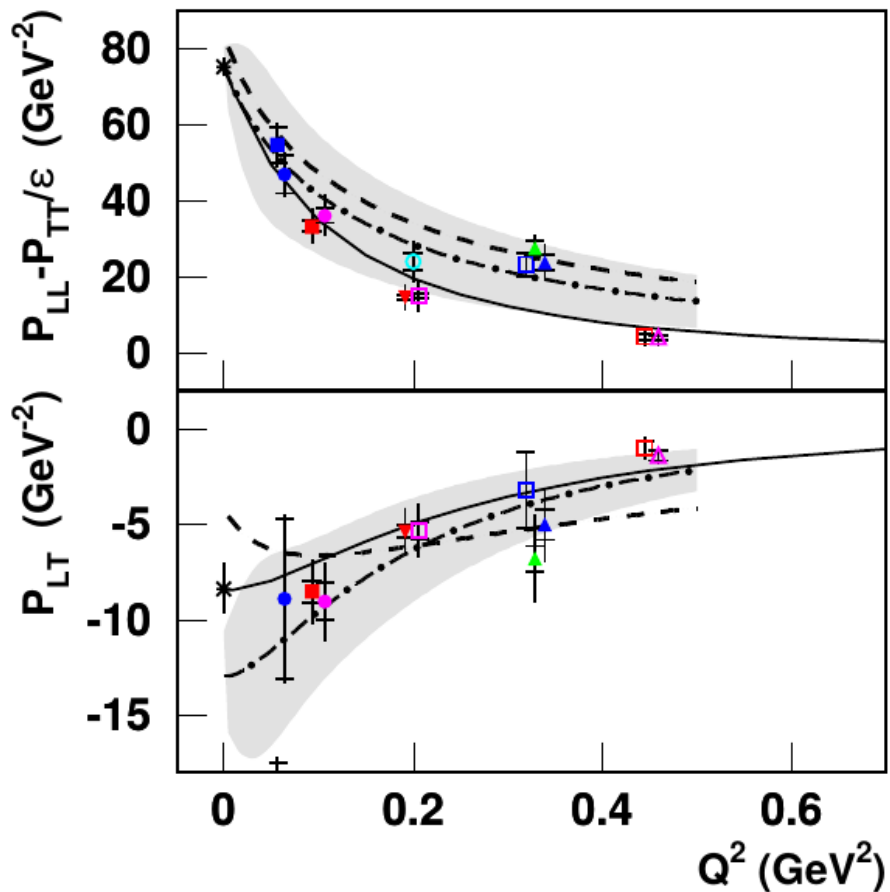


Figure 6: (color online)  $q'_{cm}$ -dependence of the cross section and the GP effect at fixed  $Q^2 = 0.2 \text{ GeV}^2$ ,  $\epsilon = 0.9$ ,  $\theta_{cm} = 100^\circ$  and  $\varphi = 180^\circ$ . Top-left plot: the LEX cross section (solid) and BH+Born cross section (dashed). Top-right plot: the GP effect from the LEX,



The solid curve is the DR model calculation for  $(\Lambda_\alpha = \Lambda_\beta = 0.7 \text{ GeV})$

$$\text{const in DR} = f(0)/(1 + Q^2/\Lambda^2)^2$$

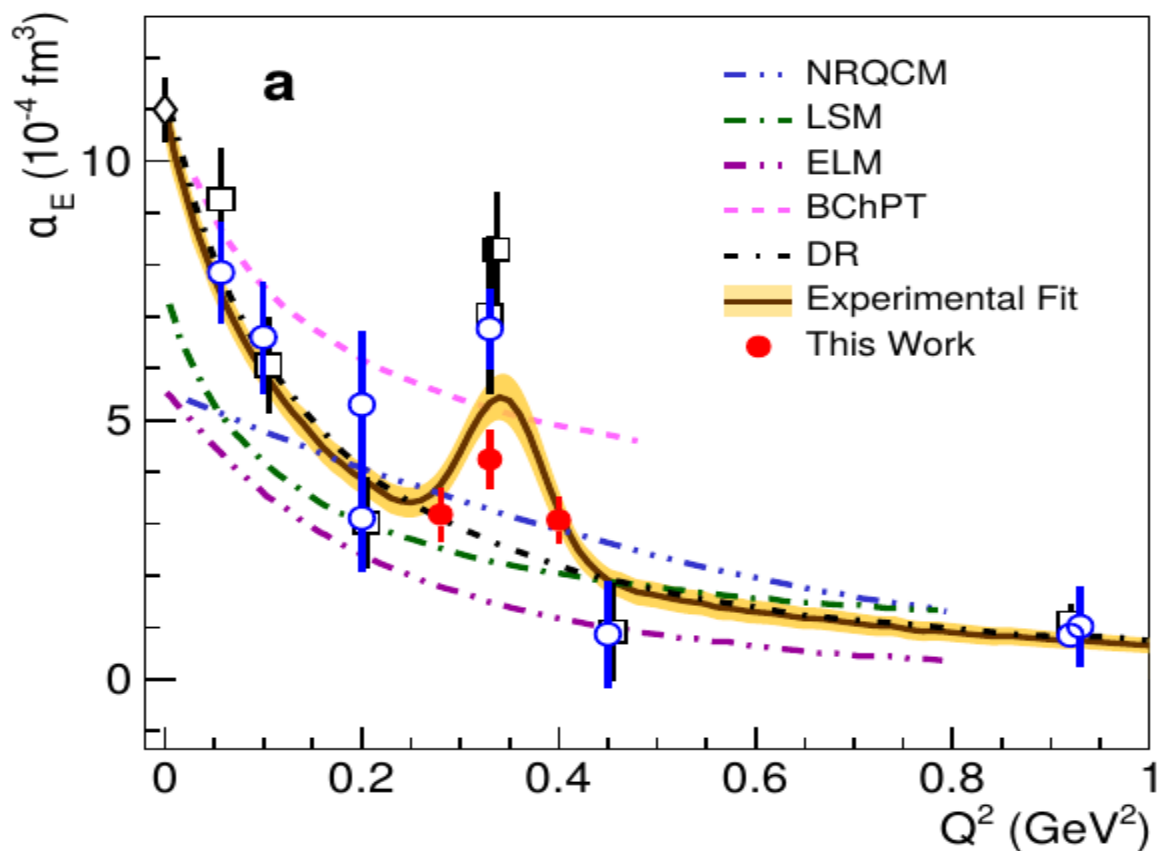


the nomenclature of Fig. [14](#). The solid curve is the DR model calculation for  $(\Lambda_\alpha = \Lambda_\beta = 0.7$  GeV). The dashed curve is the HBChPT  $\mathcal{O}(p^3)$  calculation of Ref. [34](#). The dashed-dotted curve with its error band (shaded area) is from covariant BChPT at  $\mathcal{O}(p^3) + \mathcal{O}(p^4/\bar{\Delta})$  [36](#). Right plots: the DR model calculation [39](#) for three different choices of the dipole mass parameter:  $(\Lambda_\alpha = \Lambda_\beta) = 0.5$  GeV (dotted curve), 0.7 GeV (solid curve), 0.9 GeV (dashed curve). Model calculations use  $\epsilon = 0.65$ .

$$\alpha_{E1} = 2 \sum_{N^* \neq N} \frac{|\langle N^* | D_z | N \rangle|^2}{E_{N^*} - E_N},$$

$D_z$  is the electric dipole moment operator and  $N^*$  indicates a nucleon resonance.

$$\begin{array}{ll} \Delta(1700) & J^P = \frac{3}{2}^- & Br(N\gamma) = 0.2 - 0.6\% \\ N(1680) & J^P = \frac{5}{2}^+ & Br(N\gamma) = 0.2 - 0.3\% \end{array}$$



THANK YOU